Journal of Atmospheric and Solar-Terrestrial Physics 181 (2018) 55–67

Contents lists available at ScienceDirect

Journal of Atmospheric and Solar-Terrestrial Physics

journal homepage: www.elsevier.com/locate/jastp

Solar wind diamagnetic structures as a source of substorm-like disturbances

V.A. Parkhomov[a,*], N.L. Borodkova[b], V.G. Eselevich[c], M.V. Eselevich[c], A.V. Dmitriev[d], V.E. Chilikin[a]

[a] Baikal State University, Irkutsk, Russia
[b] Space Research Institute of Russian Academy of Sciences, Moscow, Russia
[c] Institutes of Solar-Terrestrial Physics of Siberian Branch of Russian Academy of Sciences, Irkutsk, Russia
[d] Institute of Space Science, National Central University, Chung-Li, Taiwan

ARTICLE INFO

Keywords:
Diamagnetic structures
Solar wind transients
Slow solar wind
Solar wind
Magnetoshere coupling
Sawtooth substorms

ABSTRACT

The purpose of this study is to generalize the results of investigation of the magnetosphere response to two types of diamagnetic structures. Type 1 is related to sporadic SW, type 2 - to the quasi-stationary "slow" solar wind (SW). First, we consider the Type 1 of diamagnetic structures that are connected with sporadic SW, whose source on the Sun is coronal mass ejections (CMEs). Near the rear side of a magnetic cloud, one often observes a thin magnetic rope with a high-density plasma. This rope is ejected by a filament (or an eruptive prominence) from the solar surface. The rope is a diamagnetic structure with the same properties, as those of a magnetic tube. Such tubes are diamagnetic, i.e., a diamagnetic current flows on their surface. This current decreases the magnetic field inside the pipe and increases the latter outside. The total pressure (magnetic plus gas-kinetic) is approximately constant inside and outside the tube. Tubes keep their angular size during propagation from the Sun to the Earth, i.e., they are quasi-static. Type 2 represents magnetic tubes (in general case, magnetic ropes) whose sources on the Sun are the streamer belt and the streamer chains or pseudo-streamers. In the Earth orbit, the SW diamagnetic structures are detected by the presence of anti-correlation between the SW proton density and the magnitude of interplanetary magnetic field (IMF). The analysis showed that an interaction of diamagnetic structures (DSs) with the Earth magnetosphere generates substorm-like (sawtooth) magnetic disturbances in the nightside magnetosphere. The disturbances are different from classical substorms because of the absence of the growth phase and of the breakup. The diamagnetic structures related to the quasi-stationary slow SW cause a global modulation of the magnetic activity and of the ionospheric currents with a period close to the period of the variations in the SW plasma density and in the IMF strength inside the diamagnetic structure.

1. Introduction

By now, several types of magnetospheric substorms have been established depending on the solar wind (SW) conditions and on the character of its interaction with the magnetosphere. The "classical" isolated substorms having three phases (growth-expansion-recovery, Akasofu, 1971) have been studied most completely. The second type of substorms includes those having double or multiple onsets referred to as pseudo-breakups (Koskinen et al., 1993). Zhou and Tsurutani (2001) analyzed the pseudo-breakup concept in detail. In that paper based on previous investigations, the authors define a pseudo-breakup as a slight, localized brightening in the midnight sector of the auroral oval. The brightening is accompanied by a slightly localized magnetic bay. Pseudo-breakups may manifest themselves at the substorm growth phase, but, for some reasons, they may not proceed into the expansion phase. The authors believe that a primary factor (*we underline this especially*) determining the emergence of substorm is the energy accumulation in the magnetotail. That accumulation should persist for no less, than one and half hours before the shock arrival. The third type is sawtooth events. Such a term was introduced by Henderson et al. (2006), but the substorms of this type (62 events) were most comprehensively investigated by (Troshichev O.A. et al., 2010, Troshichev O.A. and Janzhura A. 2012). A key feature of such substorms, in contrast to the other two types, is the absence of the growth phase and of the breakup.

Analysis of the August 1, 1998 events (Parkhomov et al., 2011) showed that there was no growth phase in that substorm, and variations in the solar wind pressure caused a synchronous response in geophysical phenomena observed on the Earth, in the orbit of the Polar satellite, in geosynchronous orbit, and in the plasma sheet. Therefore, this

* Corresponding author.
E-mail address: pekines_41@mail.ru (V.A. Parkhomov).

https://doi.org/10.1016/j.jastp.2018.10.010
Received 23 November 2017; Received in revised form 13 March 2018; Accepted 11 October 2018
Available online 15 October 2018
1364-6826/

substorm may be referred to type-3, sawtooth events. The substorm was caused by interaction of the magnetosphere with a structure, in which the jump in SW plasma density anticorrelated (R ~ −0.92) with the strength of interplanetary magnetic field (IMF).

Similar patterns in the dynamics of the SW density and IMF strength were observed in magnetic clouds, a part of sporadic solar wind in the Earth orbit (Parkhomov et al., 2015). It was found sharp anti-correlated (R ~ - 0.9) jumps of the SW density and IMF strength while the SW velocity was almost constant. The structures were identified as diamagnetic structures (DSs). They are originated from the solar photosphere and transported by the solar wind to the Earth orbit.

DSs represent magnetic tubes (in the general case, magnetic ropes) with plasma. Such tubes are diamagnetic, i.e. diamagnetic current flows on the surface of a tube such that it decreases(increases) the magnetic field inside(outside) a tube. The tubes maintain their angular size during the Sun-to-Earth propagation, i.e. they are quasi-static throughout whole their track (Eselevich and Eselevich, 2005). The SW diamagnetic structures feature sharp and large jumps of the SW pressure and they are distinguished by the anti-correlation between the SW density and IMF strength.

Hitting the Earth magnetosphere, DSs may cause short-time (20–40 min) activations of magnetospheric processes similar to substorm ones (Parkhomov et al., 2015). They start on the dayside as shock auroras in the noon sector (Zhou and Tsurutani, 1999). Herewith, unlike classical substorms, the DS forcing on the magnetosphere also manifests itself in the cases, when long-living IMF Bz component preceding a magnetospheric disturbance may be positive or weakly negative. 3–5 min after a shock aurora occurred on the day side, some phenomena inherent in a substorm are observed at the Earth on the night side and in the magnetotail: bursts in Pi 1–2 geomagnetic pulsations, an increase in the electron and proton fluxes in the geosynchronous orbit, and an increase in the auroral electrojet (the AE-index grows to 600 nT, and, in cases of especially strong jumps of SW density in a DS, the AE-index may reach ~1000 nT). The duration of magnetospheric disturbance is determined by the time of interaction between the DS and the magnetosphere.

The goal of this study is to generalize the results of investigations of magnetospheric responses to diamagnetic structures. We selected and analyzed the events, in which a long-living positive (or weakly negative) IMF B_z component preceded the DS collision with the magnetosphere, i.e. there was no preliminary energy accumulation for the substorm in the magnetotail.

First, we address the sources of diamagnetic structures on the Sun, trace their features in the solar wind, and, then, we describe the effects of interaction of such structures with the magnetosphere.

1.1. Two types of SW diamagnetic structures

Investigations of the last several decades showed the existence of two types of DSs in the solar wind: type 1 is related to the sporadic SW, type 2 is associated with the quasi-stationary slow SW.

We address sequentially each of these types.

Type 1 is related to the sporadic SW. Its source on the Sun is coronal mass ejections (CMEs), Fig. 1. The latter are detected in the Earth orbit in the form of a sequence comprising a shock, shock-heated plasma, and a magnetic cloud, or an interplanetary coronal mass ejection (ICME). Inside a magnetic cloud, one often observes a bending thin magnetic rope with higher-density plasma. This thin rope is a filament (or an eruptive prominence) ejected from the solar surface, Fig. 1. It is a diamagnetic structure with the same properties as those for a magnetic tube of the quasi-stationary slow SW (Eselevich and Eselevich, 2005).

Type 2 forms the basis of the slow quasi-stationary SW in the Earth orbit. Its sources on the Sun are a belt of streamers (Svalgaard et al., 1974) and chains of streamers (Eselevich et al., 2007; Eselevich et al., 1999), or pseudo-streamers (Wang, Y.M.; 2007). Herewith, the slow SW features a relatively low velocity in the Earth orbit V ≈ 250 ÷ 450 km/s (in the fast SW streaming from coronal holes, the velocity is V ≈ 450 ÷ 800 km/s) (Eselevich and Fainshtein, 1991).

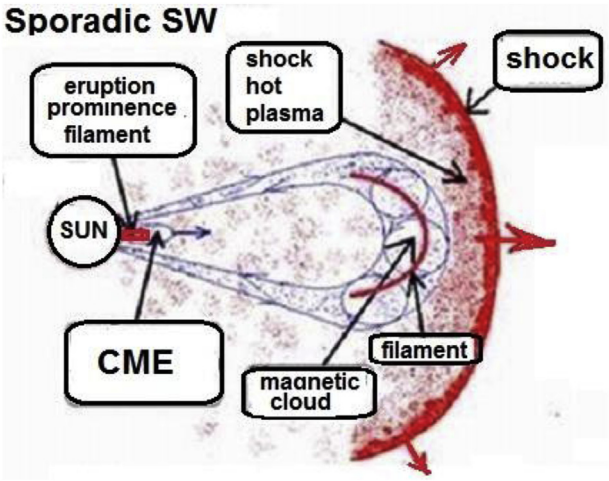

Fig. 1. A scheme of propagation of a sporadic solar wind structure from the Sun to the Earth in the ecliptic plane as seen from the Northern pole.

On the solar surface, the streamer belt separates the regions with the opposite direction of the radial component of the global magnetic field (Svalgaard et al., 1974). This implies that, at the streamer belt basis, there are magnetic field arches, through the tops of which there transits the neutral line (NL) of the radial component of the solar global magnetic field of the Sun. Fig. 2A shows a sequence of loops (with the inscription" Streamer belt ") crossing the solar equator, and the neutral line is indicated by the dashed curve connecting the tops of the loops. Fig. 2b shows a cross-section of the streamer belt, at the base of which an arched structure or "streamer helmet" is visible. The arched structure is manifested by the loops shown in Fig. 2A.

The structure of the coronal streamer belt above the “helmet” consists in a sequence of pairs of rays with increased brightness (density) or two closely located rows of rays (see Fig. 2a). The neutral line passes between the rays of each pair along the belt (as shown by the solid curve in Fig. 2a) (Eselevich and Eselevich, 2006).

The rays structures forming the belt, in fact, are magnetic tubes (in general, magnetic wisps) with a plasma of increased density (or increased gas-kinetic pressure) (Eselevich M. and V., 2005). Such tubes are diamagnetic, i.e. a diamagnetic current flowing at their surface decreases the magnetic field inside and increases outside the tube. The total pressure (magnetic plus gas-kinetic), is approximately constant inside and outside the tube. The tubes retain their angular size during propagation from the Sun to the Earth, i.e. they are quasi-static throughout this entire path (Eselevich and Eselevich, 2005).

The portion of intersection of the neutral line with the solar equator (the horizontal straight line in Fig. 2A) is observed at the Earth's orbit as a sector boundary of the interplanetary magnetic field (IMF) (Korzhov, 1977). In Fig. 2B, the sector boundary corresponds to a change in the azimuth angle of the IMF by 180°, as marked with the inscription “The IMF sector boundary”. In Fig. 2A and B, the correspondence of parts of the sector boundary is shown by the large arrow with the inscription “sec".

Streamer chains in the corona appear (in white light), like the streamer belt, in the form of a sequence of bright (dense) beams. They bring the slow SW with approximately the same properties as those in the streamer belt. However, the streamer chains differ from the streamer belt because in the corona, they separate the regions with the open magnetic field lines having the equal polarity (Eselevich et al., 2007). Therefore, the magnetic field structures at the basis of the chains calculated in the potential approximation appear like double arches (in general case, an even number of arches), whose tops are shown by the dotted line in Fig. 2a).

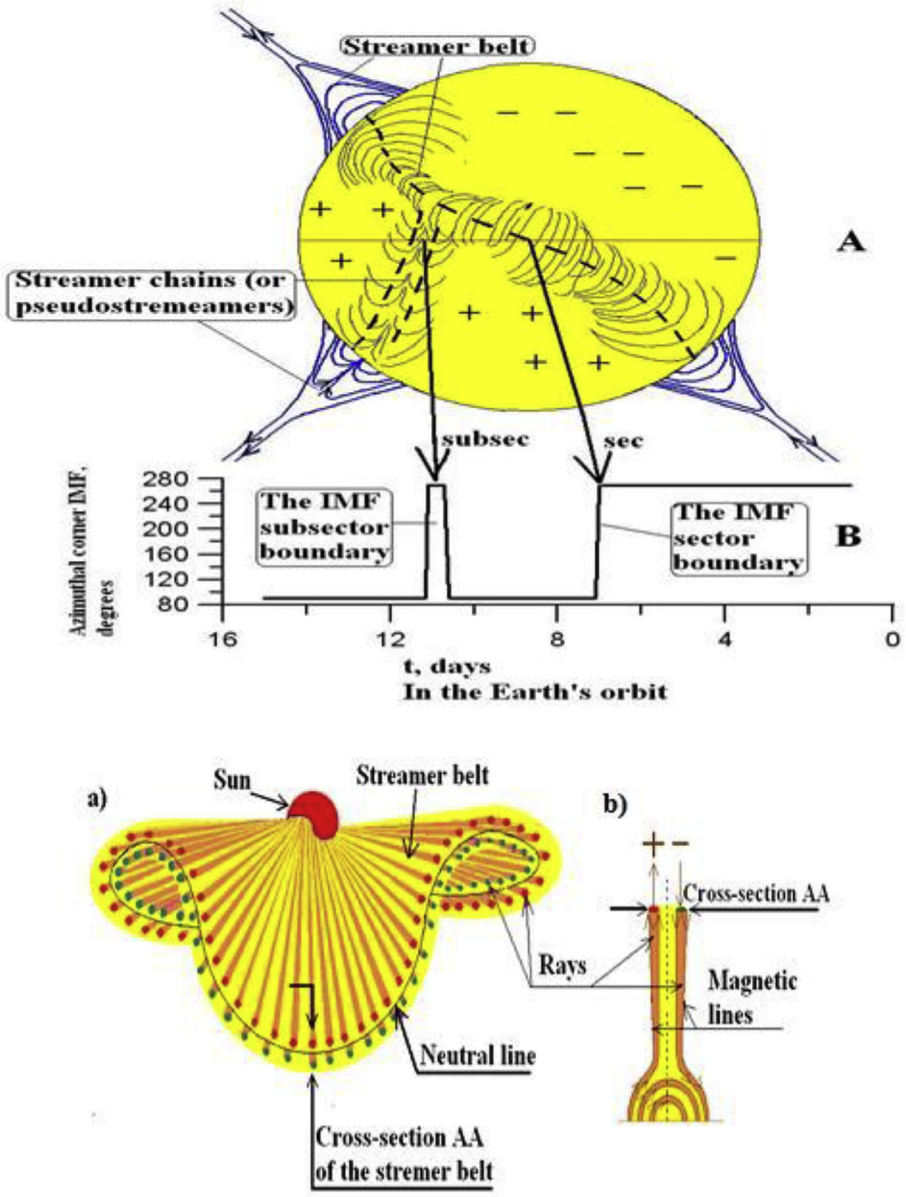

Fig. 2. A) A scheme for the magnetic field lines at the basis of the streamer belt and of the streamer chains separating the regions on the Sun surface with the opposite and equal directions of the Sun global magnetic field radial component, respectively. Single dotted line is the neutral line of the magnetic field radial component. The NL transits on the tops of the magnetic field arcs at the belt basis. Double dotted line is two neutral lines along the magnetic field dual arcs at the basis of the streamer chains. B) A scheme for distribution of the azimuth angle of interplanetary magnetic field (IMF) in the Earth orbit at the Sun's rotation along the red line (ecliptic) on (A). a) Spatial beam structure of the coronal streamer belt. b) Cross-section (AA) of the streamer belt. In the red beams of the upper row of the streamer belt, the magnetic field is directed from the Sun (+), in the green beams of the lower row, the magnetic field is directed to the Sun (−). The neutral line is between the beams (solid line).

In the Earth orbit, the streamer chains can be found in the form of high-density plasma streams containing an even number of changes in the IMF polarity. Those streams are referred to as subsectorial IMF boundaries (shown by the “subsec” arrow in Fig. 2a., Ivanov et al., 2002). Herewith, the beams of both the belt and the chains of streamers representing quasi-stationary diamagnetic structures of the slow SW can be revealed from the presence of a negative correlation between the jumps in SW density N and IMF strength B.

In Fig. 2A they are shown by a sequence of pairs of loops (with the inscription "Streamer chains or pseudostremers") crossing the solar equator, and their tops - by two dotted curves.

At the Earth's orbit, a portion of intersection of the streamer chain with the solar equator is observed as a region with an increased density of plasma containing an even number of changes in the sign of IMF, which is called a subsector boundary of IMF (Ivanov et al., 2002). In Fig. 2B, the subsector boundary corresponds to a double change in the IMF azimuth angle by 180° and back to - 180°, as marked with the inscription “The IMF subsector boundary”. In Fig. 2A and B, the correspondence of parts of the subsector boundary is shown by a large arrow with the inscription “subsec".

In this case, the rays of the belt and streamer chains, which are quasi-stationary diamagnetic structures of the “slow” SW, are determined by the presence of a negative correlation between the jumps in the solar wind density N and the IMF strength.

2. Diamagnetic structures related to sporadic solar wind streams

2.1. Analysis of observations on the Sun and of the sporadic SW streams in the Earth orbit on June 28, 1999

We consider the features of the June 28, 1999 sporadic SW streams between ~03:30 UT and 05:12 UT (Fig. 3I). Its source on the Sun was a halo CME (HCME that originated on June 26, 1999 at ~07:31 UT (heliocoordinates N25E00).

This specific sporadic SW stream between about 03:30 UT and 04:48 UT on 1999 June 28 presented in Fig. 3I may be characterized as a small interplanetary transient (SIT). Indeed, an SIT is a small-size ICME, whose duration is usually significantly longer, lasting 0.5–1.5 days. According to (Rouillard et al., 2011), SIT has following features in the Earth orbit:

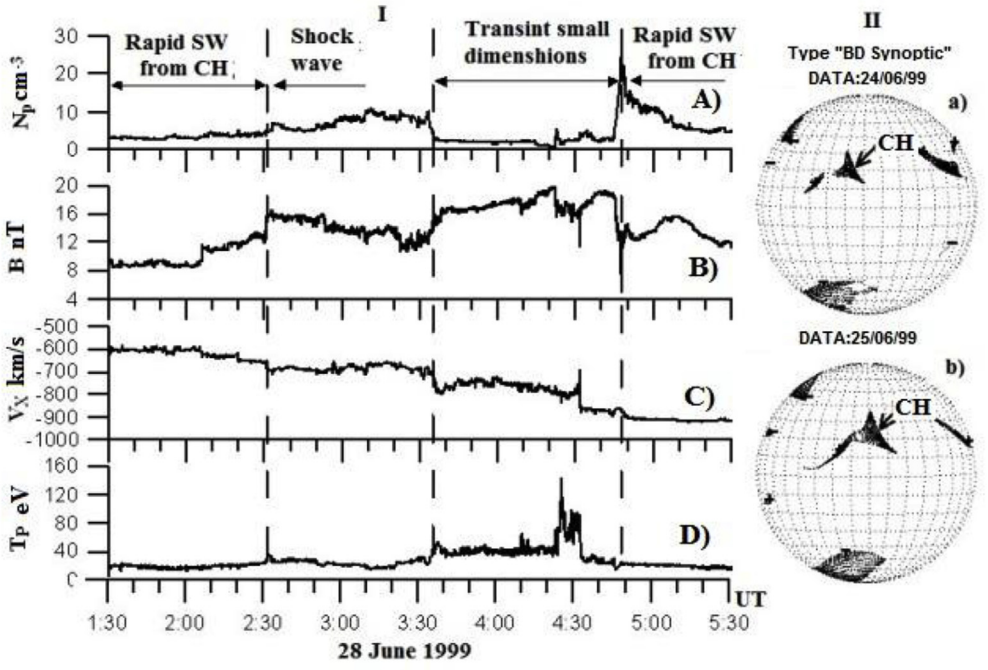

Fig. 3. (I) Variations of the solar wind parameters on 28 June 1999 according to the WIND satellite data: a) plasma density, b) IMF strength, c) velocity along the Sun-Earth line, d) proton temperature. (II) The results of Rudenko's calculations (http://bdm.iszf.irk.ru/.) in the potential approximation of the positions of the bases of open magnetic tubes corresponding to coronal holes (CH). The image (a) is given at 14:28 UT 24 June 1999, (b) - at 14:28 UT 25 June 1999. Symbols "plus" and "mines" indicate the direction of the magnetic field outward and toward the Sun, respectively.

1) Decrease or increase in the polar (latitude) angle θ of the magnetic field B during $\sim 1 \div 10$ h (Fig. 3(I)f).
2) Fast decrease in the plasma parameter $\beta = 8\pi P/B^2$ (β is the ratio of thermal to magnetic pressure) to $\beta << 1$ Fig. 3(I)g associated with a sharp increase of B at the boundary and reduction in SW density N_p (Fig. 3(I)a,b).

A SIT usually propagates in the slow quasi-stationary solar wind, whose velocity in the Earth orbit is $V_{sw} \leq$ 400–450 km/s. Herewith, the SIT rear part often represents an N_P density peak, whose profile anti-correlates with the profile of the magnetic field B. Such a structure of the SW density profile and of the IMF strength is diamagnetic. According to (Rouillard et al., 2011), a source of the SIT diamagnetic structure near the Sun is an eruption process of a streamer basis helmet top (or the top of a streamer arch structures). While moving, this N_P peak may be intensified (and accelerated) due to its compression by the chasing fast streams of the quasi-stationary solar wind (Rouillard et al., 2011).

As one can see in Fig. 3I, the June 28, 1999 event meets the above requirements at ~03:30 UT - 04:48 UT (marked by vertical dotted lines in Fig. 3I). But it has very important feature: this SIT propagates over quasi-stationary fast SW, whose velocity is $V_{sw} \approx$ 600 km/s. The source of the fast SW is a coronal hole (CH), whose center intersects the central meridian on June 25, 1999. This conclusion follows from the calculation by Rudenko (http://bdm.iszf.irk.ru/) of the magnetic field in the corona from the measurements of photospheric magnetic field. The arrow in Fig. 3(II) indicates the calculated position of the CH open magnetic tube basis. From Fig. 3(II)b it follows that the center of this CH intersected the central meridian between 0 and 14 UT on June 25, 1999 at $\theta_0 \approx 25^\circ$. The estimate of the CH tube basis area in Fig. 3(II)b yields the value of $S \approx 5.5 \cdot 10^{10}$ km^2. This enables to estimate the maximal velocity, V_M, of the SW stream from this CH at 1 AU and determine the time moment t_M, when the SW stream from this CH arrives the Earth by the following expressions (Eselevich et al., 1999):

$$V_M(S, \theta_0) = \{(2.25 \bullet 10^{-9} S + 500) - 4[\text{km/(s·deg)}] \cdot (|\theta_0 - B_0|)[\text{deg}]\}, [\text{km/s}] \quad (1)$$

$$t_M (V_M) = t_0 + 236.5 R_0 / V_M, [\text{sec}] \quad (2)$$

where B_0 is the Earth heliolatitude, S is in (km^2), R_0 is the solar radius.

The estimate provides: $V_M \approx$ 590 km/s, the t_M varies within the 07–21 h range on June 28. The V_M velocity value agrees with the observed value of the fast SW from this CH over the first hours on June 28, and the calculated value t_M corresponds to the observation accuracy within ± 12 h (Eselevich et al., 1999).

At the same time, as seen in Fig. 3(I)d, after 5 h on early June 28, 1999, directly after the SIT, one observes an increase in the velocity of fast SW from the addressed CH. That it is the quasi-stationary SW from CH evidences a relatively small value of $N_p < 10$ cm^{-3} and the characteristic value of the magnetic field B ≈ 4–5 nT (within, at least, 06:30–18:00 UT on June 28, 1999 from the *WIND* data, but they are not shown here) at the maximal velocity $V_M \approx$ 900 km/s. The only difference is the stream duration that, at the semi-height V_M is near $\Delta t \approx$ 12 h (from the *WIND* data), whereas the typical value Δt for fast streams with $V_M \approx$ 600–900 km/s is within 3–5 days.

It is possible to elucidate such an increase in V_M, as long as one admits that the June 25 area S of the CH magnetic tube basis was increased within several hours by approximately a factor of 3 after intersection of the central meridian. Herewith, according to Formula (1), the velocity of the fast SW from this hole should grow up to ~850 km/s. Such an increase in S was quite possible, because in the previous day between 24 and 25 June 1999, the CH area S had already changed (increased by more, than a factor of 2 in Fig. 3 II).

In summary, the uniqueness of the addressed case is in that the HCME that originated at ≈07:31 UT on June 26, 1999 (heliocoordinates N25E00) and was accompanied by the filament eruption, underwent a forcing from the fast SW, whose velocity reached an extremely high value of almost 900 km/s.

The sequence of the process appears like the following. According to [http://cdaw.gsfc.nasa.gov/CME_list/] at R ≈ 20R$_0$, the HCME had the velocity in the sky plane $V_\perp$ = 400 km/s, and underwent a deceleration with the rate of a = −9.8m/s^2. This implies that its velocity in the radial direction did not exceed $V_R \approx 1.8 V_\perp \approx$720 km/s according to (Schwenn et al., 2005). That velocity was also continuously decreasing due to the CME deceleration during the expansion toward the Earth.

However, as long as, the area of the CH magnetic tube basis increased for several hours by approximately a factor of 3, upon intersection the central meridian on June 25, 1999, then the velocity of the

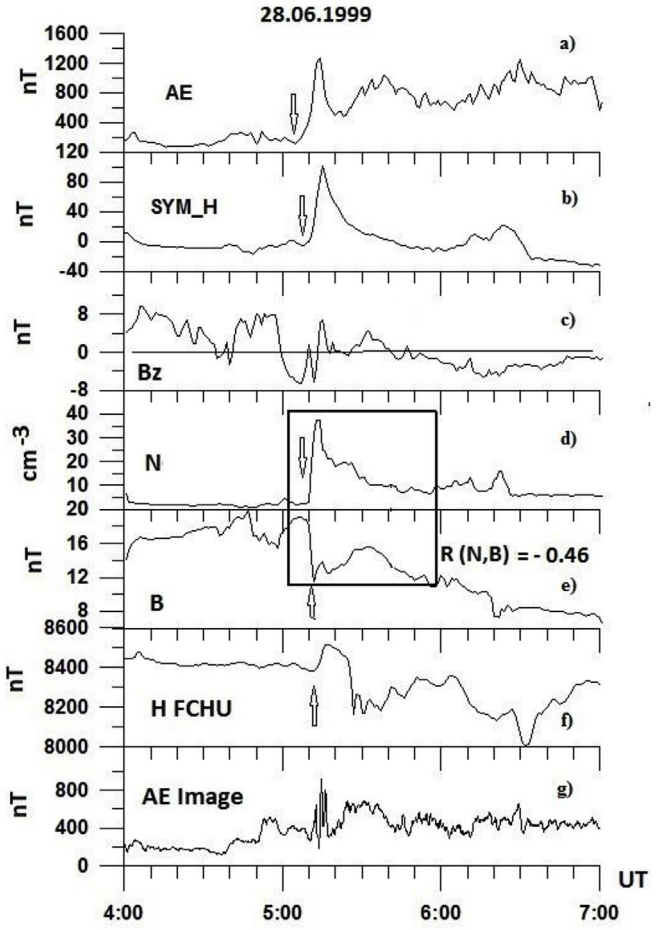

Fig. 4. Magnetospheric response to the June 28, 1999 diamagnetic structure (from top to bottom): a) variations in the AE index, b) variations in the SYM-H index, c) variation in the IMF Bz component, d) variation in the SW density, e) variation in the IMF strength, f) fragment of the FCHU Observatory magnetogram (Φgm = 69°, 7) at the local midnight (MLT = UT - 6,4), g) local AE index from the IMAGE magnetometer network located on the dawn side (MLT = UT +1.2). The diamagnetic structure is denoted by the rectangle, and the arrow marks the onset of the DS coupling with the magnetosphere.

fast SW from the hole could increase up to ≈900 km/s. As a result, the CME with the diamagnetic structure (filament), having comparatively low velocity, was overtaken and dragged by the fast SW, and then it was detected in the Earth orbit like a SIT moving with $V \approx 900$ km/s.

2.2. Magnetospheric response to the June 28, 1999 diamagnetic structure

The magnetospheric response to a diamagnetic structure can be detected by variations in the planetary and local (obtained from a limited magnetometer network) indices of magnetic activity. Fig. 4 shows the variations in the indices, in the SW parameters, and in the IMF. There is also a fragment of the magnetogram from the observatory located at near-midnight hours of local time, when the DS hits the magnetosphere.

As seen in Fig. 4, the interaction results in a sharp global increase in the magnetic activity. The main feature is the evolution of phenomena proper for an auroral substorm in the near-midnight sector. We draw attention to this, because, prior to the disturbance onset, the IMF vertical component had great positive values within 5 h (Fig. 4c), while, for the negative Bz, the substorm growth phase lasts ~1 h. In the present event, Bz had the southern direction for only 10 min (Fig. 4) before the DS arrival. The AE index, characterizing the magnetic activity in the auroral region, reached 1200 nT and then persisted at ~800 nT during the interaction of DS with the magnetosphere.

Fig. 5 presents the dynamics features for the energetic particle precipitations and the auroras observed by the Polar satellite with the LBHL (Lyman-Birge-Hopfield long 155–188 nm) and LBHS (Lyman-Birge-Hopfield short 140.0–150.0 nm) filters. The satellite was in the noon region of the magnetosphere at geocentric distance ~4 Re at 04–06 UT June 27, 1999.

An abrupt increase of the electron flux in the 10^2–10^3 eV energy range and of the proton flux in the 10^3–10^4 eV energy range started at 0512 UT (Fig. 5a). This time moment coincided with a sharp increases of H-component at the observatories of the noon meridian (the SYM-H index reached ~100 nT in Fig. 4), and with the start of intense geomagnetic pulsations recorded in the Pc1 frequency range (Tsegmed, 2002). The pulsations are originated from precipitations of energetic proton (the arrow in Fig. 5a).

Electron precipitations cause activation of auroras. On the sequential frames in Fig. 5b, one can see that after the initial brightening at 5:00:07 UT at the latitudes of the daytime polar cusp (~72°÷76°) at 0511:46 UT, a strong brightening occur near the noon meridian, and the glow forefronts move onto the dawn and dusk sides. One can see clearly a displacement of the glow eastern edge in Fig. 5b (Frame 0516:04 UT), where the glow front reached the premidnight sector (~02h), and, in Fig. 5c, one can see a joining of the glow boundaries at the midnight meridian (Frame 0518:12 UT). At 0523:43 UT, it is apparent that the glow encompasses the entire auroral oval that is one of the main substorm signatures.

From the ground-based observations by zenith photometers at the midnight meridian (GILLIAM Observatory), an abrupt (by a factor of 10) increase in the 486 nm glow intensity starts at 67° latitude at ~0514:30 UT, i.e. ~3 min after the sharp increase in the glow brightness on the dayside (Fig. 5d). Like shown by (Zhou and Tsurutani, 1999), the propagation velocity of the shockaurora forefront toward dawn and dusk is determined by the shock velocity along the magnetopause and it is 6–11 km/s. In the present case, the glow onset on the nightside is observed ~3 min after the glow increase on the dayside. Probably, such a small lag may be associated with a high propagation velocity (~900 km/s) of the diamagnetic structure in the solar wind.

Another confirmation of the generation of the substorm disturbance caused by the interaction with DS is the variations in the geomagnetic field detected by GOES-8 in geosynchronous orbit. The sequence of the response phenomena in the quasi-trapped region in the nightside magnetosphere is the following. First, a sharp increase of H-component was caused by an increase in the Chapman-Ferraro currents at the magnetopause and by the magnetosphere compression (Line 1). Then, GOES-8, located in the quasi-trapped outer magnetospheric region near the midnight meridian, detected variations in the Bz and Bx components of the geomagnetic field (rectangles II, III in Fig. 6a and b). The variations are characteristic of the geomagnetic field dipolization. This is one of the main signatures of a substorm (Sergeev et al., 2012; Lui, 2001).

All the above allows us to believe that the power source for the substorm-like phenomenon in the magnetosphere is a DS in the fast SW stream. We obtained a similar conclusion in the analysis of substorms on August 1, 1998 (Parkhomov et al., 2011). The intervals in solar wind, where the density variations anti-correlated with the IMF strength, were established to be a cause of synchronous response in the geophysical phenomena observed on the Earth, in the orbit of Polar satellite, in the geosynchronous orbit, and in the plasma sheet. A jump in the SW pressure under weakly negative IMF Bz, whose amplitude increases at the jump, may be not only the substorm trigger, but it can also further determine the release of the energy arriving from the solar wind.

Zhou et al. (2013) considered a similar model for the SW pressure jump forcing. According to the model, the jump of the SW density and of the IMF strength may be identified as a DS. The structure propagates with a high speed solar wind along the magnetotail and compresses the

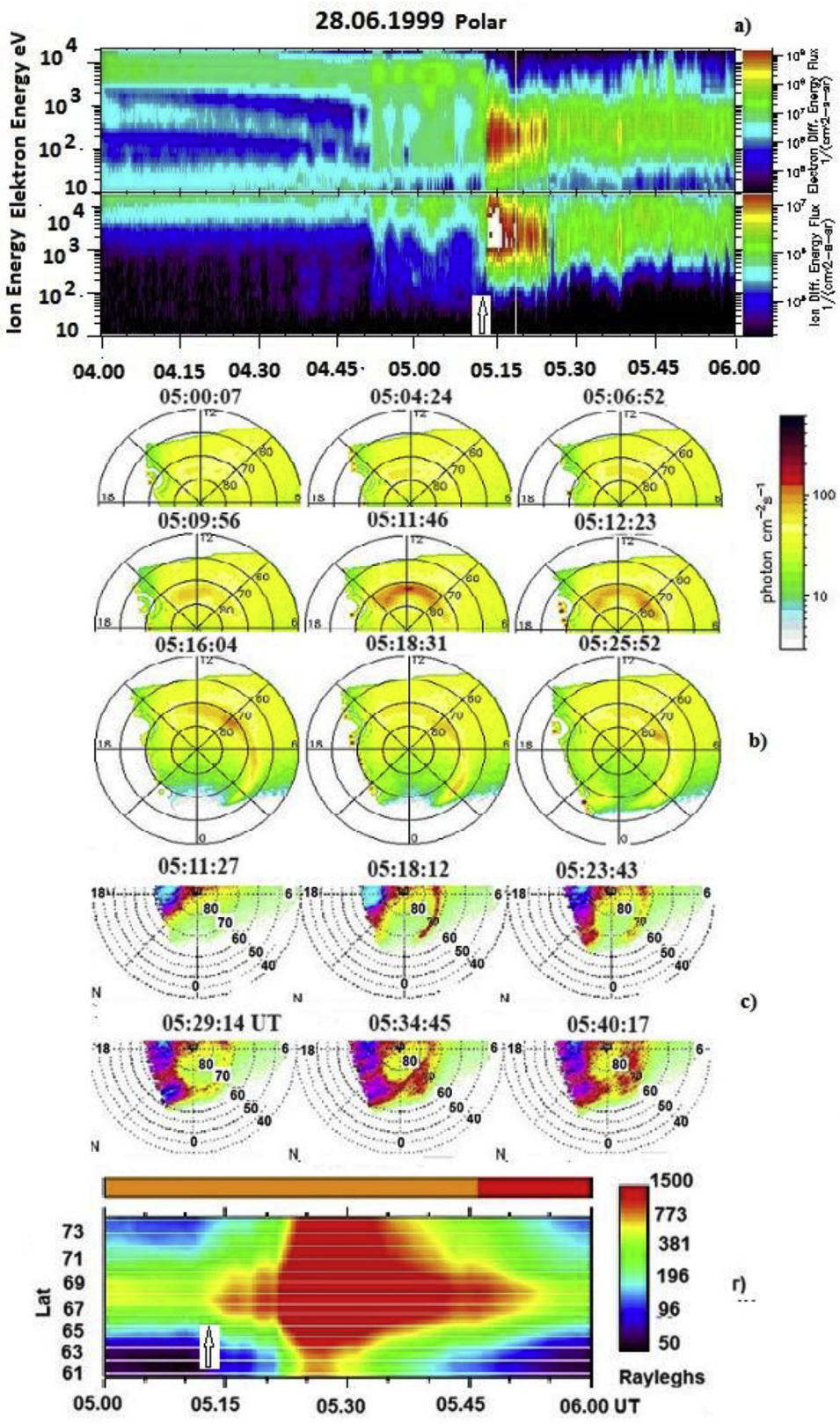

Fig. 5. Variations in the electron and proton fluxes near the noon meridian from observed by the Polar satellite, b) sequence of the LBHL-filtered images of glows from the Polar satellite, c) the same interval of observations, but by using the LBHS filter, d) the data from the ground-based zenith photometer near the midnight meridian MLT ~23:00 (CILLIAM). The arrow in Fig. 5a denotes the instant of a sharp increase in the particle flux and the onset of the increase in aurora brightness at the noon meridian.

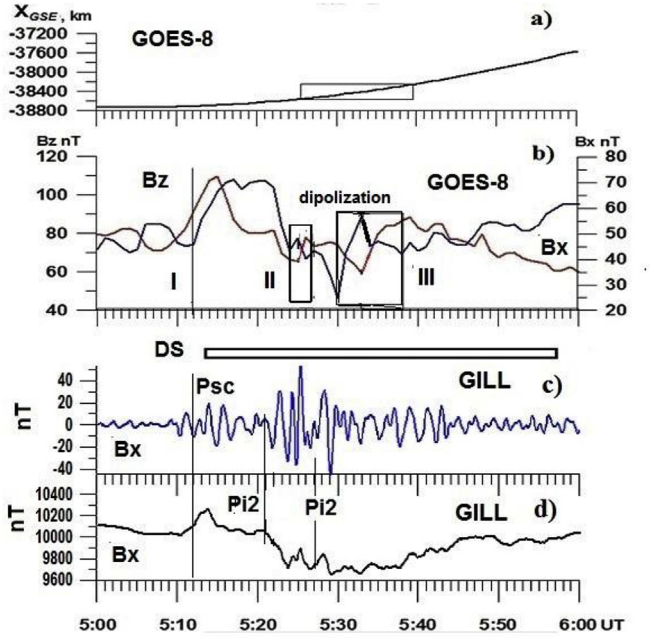

Fig. 6. Variations in Bz and Bx geomagnetic field components measured by GOES-8. a) The satellite orbital position during the coupling with the DS; b) I denotes the onset of the glow increase at the noon meridian, II, III denote the instants of the onset of the Bz, Bx anti-phase motion in the magnetic field at geosynchronous orbit (dipolization intervals).

tail magnetosphere. This results in the energy transport to the plasma sheet and in the evolution of the processes similar to those occurring during a classical substorm. After the tail thinning down to 80% (Zhou X., 2013), earthward plasma flows and dipolization fronts appear similarly to those in Fig. 6b. These phenomena lead to the processes in the auroral region, which are similar to an auroral substorm.

A peculiarity of the present event and its difference from a shock-aurora is a weak increase of the glow at ~73–78° latitudes observed at 0500:07 UT in the near-noon sector within 11–13 MLT, which starts at the same time when Bz changes its direction from northward to southward. But the sharp increase of glow occurs later, at 0511:46 UT, at the moment of the jump in the SW density and the Bz turning northward (Fig. 4). Therefore, in the present case, one cannot deny the role of magnetic reconnection in the energy transport from the solar wind into the magnetosphere. A short-time existence of the southward IMF component may be likened to a valve opening the DS energy transport into the magnetosphere. But we should again emphasize that the southward orientation of IMF lasts only ~10 min, while classical studies of substorms indicate that the substorm onset should be preceded by the southward IMF orientation for ~1 h, which determines the substorm growth phase duration. One may assume that, in the present case, the growth phase of substorm-like disturbance (SLD) started at the moment of the IMF turning southward and lasted for 10 min (Fig. 4).

2.3. Inference to the DS related to sporadic SW

The diamagnetic structure in the sporadic solar wind generated a powerful substorm-like disturbance in the magnetosphere upon the long-lasting (~5 h) northward IMF. The maximal intensity of disturbance (AE = 1262 nT) is comparable with the value of a classical substorm. One may attribute the observed disturbance to a saw-tooth substorm because of the following features: the dipolization pattern of geomagnetic variations in the outer quasi-trapped region, the dynamics of the auroral absorption, the dynamics of the ionospheric current systems, and the drift of the source of the irregular geomagnetic pulsations to the midnight meridian. We provided the arguments in favor of the assumption that the disturbance involves the elements inherent in substorms in Figs. 4–6. The analysis shows that the onset of SLD is related to the DS interaction with the magnetosphere and it is accompanied with the following phenomena:

1) an abrupt enhancement in energetic particle precipitations at the noon and midnight meridians;
2) emergence of a homogeneous glow arc in the UVI range on the day side at latitudes of the cusp with its subsequent sharp brightening;
3) west- and eastward motion of the glow forefronts from the noon meridian and the subsequent joining of the glow edges in the auroral oval.

The magnetospheric disturbance caused by the diamagnetic structure lasted ~60 min.

3. Diamagnetic structures in the quasi-stationary slow SW

3.1. Analysis of observations on the Sun and parameters of the streamer belt segment in the Earth orbit on July 15–16, 1998

We consider a case of diamagnetic structure related to a segment of the streamer belt observed at the Earth orbit. To identify this segment, we use the follow reliably stated and experimentally tested provisions (Eselevich et al., 2007):

1) The source of segment on the Sun surface should be located in vicinity of the point, where the streamer belt crosses the ecliptic. On the synoptic chart in Fig. 7, the streamer belt corresponds to the neutral line (NL) separating the positive (solid curves) and negative (dotted line) polarities of the magnetic field. One can see that, at time moment t_0 = 10 July 1998, the vicinity of intersection between NL and the ecliptic passes the central meridian. This region is the source of the slow SW, whose arriving time to the Earth orbit (t_{Earth}) can be calculated.
2) The arriving time t_{Earth} for the streamer belt segment is determined by the formula (Eselevich et al., 2007)

$$t_{Earth} \approx t_0 + 4.6 \times 10^4/V(km/s), \text{ (hours)} \quad (3)$$

According to (Eselevich M. V., 2005) in the Earth orbit, the velocity of the slow SW flowing in the streamer belt can be estimated of V ≈ 350 km/s with uncertainty of several tens of km/s. The propagation time in the calculation of t_{Earth} (in according to Eq (3)) is usually assumed to be 5.5 days, which correspond to the t_{Earth} ~ 12 UT on 15 July 1998 (dotted arrow in Fig. 8c).

3) In the Earth orbit, the streamer belt segment that is usually referred to as the heliospheric plasma sheet (HPS) should feature a higher density with N > (10 ± 2) cm^{-3}, a low SW velocity V ≈ 300–450 km/s, and the presence of the IMF sector boundary inside HPS. This implies that the change in the sign of azimuth angle Φ defining the IMF direction (toward or outward the Sun) should occur an odd number of times.

As seen in Fig. 8e, the SW velocity at 1 AU is ≈ 320 km/s at the time moment derived from Eq (3). This implies that the more exact arrival time (by Formula (1)) for the segment of streamer belt at 1 AU is ≈ 0000 UT on 16 July (solid arrow in Fig. 8c). The segment features the maximal density N ≈ 47 cm^{-3} and the IMF sign changes from positive to negative value in Fig. 8c. This corresponds to the sequence of the solar global magnetic field sign change, when the NL crosses this streamer belt segment at the central meridian on July 10 (≈00:00 UT) in Fig. 3. I.e., it is, indeed, the source of the HPS site. It should be noted that the maximal value of the SW density at this HPS site is unusually great and reaches almost 47 cm^{-3} (Fig. 8d). This might be related to a

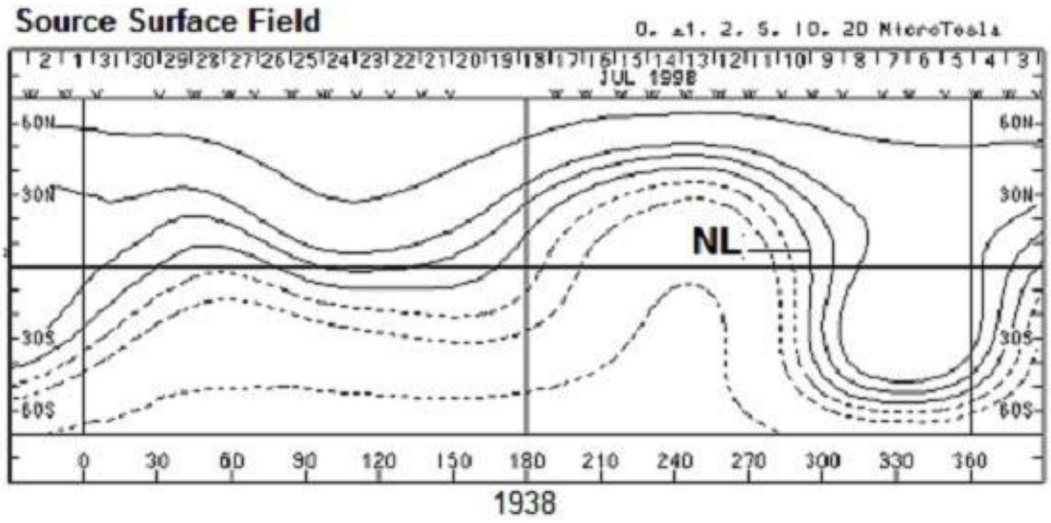

Fig. 7. Synoptic chart of Carrington Rotation 1938 for the Sun magnetic field. The chart was calculated in potential approximation (http://wso.stanford.edu/ >): solid curves are the positive polarity, the dotted line being the negative polarity. NL is the neutral line of the Sun global magnetic field.

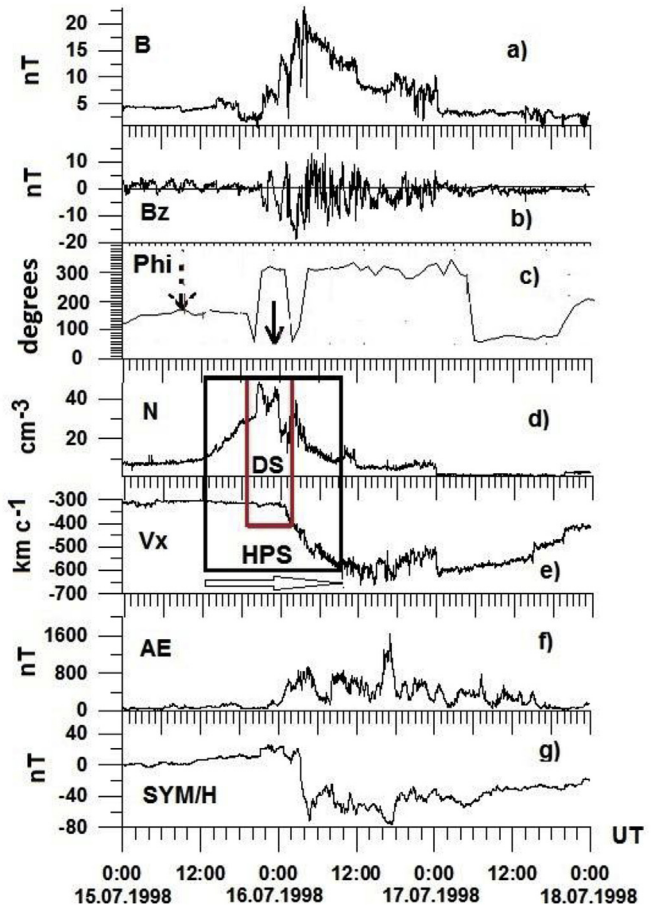

Fig. 8. Parameters of the Interplanetary magnetic field (a–c) and of the solar wind plasma (d, e) for the streamer belt segment in the Earth orbit or the heliospheric plasma sheet (the horizontal arrow shows the HPS). The rectangles denote the HPS and the CIR-related diamagnetic structure. The magnetospheric response is presented by the AE and SYM-H indices (f, g).

strong dependence of N from the angle λ of HPS inclination to the solar equator.

In fact, according to (Eselevich M. and V., 2005), there is a notion of horizontal and oblique HPS sites. Near the Sun, the angle λ corresponds to the NL inclination to the solar equator, when this site crosses the central meridian. The HPS site subtending $< 10^{\circ}$ with the ecliptic plane is referred to as horizontal, and, as long as the $\lambda > 10^{\circ}$, this site is regarded as oblique. The HPS horizontal site experiences minimal distortions, when the slow SW composing this site expands from the Sun because it does not collide with the fast SW emanating from coronal holes. On the other hand, the HPS oblique site often undergoes an additional compression (of the plasma density and the magnetic field) due to the collision with the fast SW. Herewith, the more the λ, the stronger the additional compression (Eselevich and Fainshtein, 1991).

In the present case, the NL inclination angle is maximal and is $\lambda \approx 90^{\circ}$ (Fig. 7). As a result of a strong additional compression by the fast SW, the maximal density of 47 cm^{-3} is recorded at the HPS site. (From the IMP-8 and *Geotail* data, the density N may be even more, around $\approx 70\ cm^{-3}$). In Fig. 8d, the maximal-compression site with diamagnetic properties (marked DS) is also referred to as the corotating interaction region (CIR).

3.2. Terrestrial response to the July 15–16, 1998 diamagnetic structure

According to the estimates above, the midpoint of the corotating structure should reach the Earth orbit on July 16, 1998 approximately at 0000 UT. Herewith, the HPS has a finite temporal size of about 10 h (Fig. 8d). Therefore, the observations by *Geotail* and *IMP-8* located ~4 Re upstream of the magnetopause recorded the start of the SW density growth from 45 to 70 cm^{-3} a little earlier, at 2100 UT (Fig. 9). The terrestrial disturbance caused by this structure may be defined as a small magnetic storm with a sudden commencement at 2114 UT. The storm growth phase (DCF) continued until 0000 UT on July 16, 1998 and then there was a drop in the H-component (with the minimum Dst = −46 nT at ~0500 UT) (Fig. 8g). The auroral magnetic activity increased abruptly at 0000 UT on July 16: AE reaches ~800 nT at 0340 UT and ~1600 nT at 1700 UT (Fig. 8f).

A sudden commencement in the form of the jump in H-component at the bulk of the Intermagnet observatories manifested itself in the growth of SYM-H index from 11 to 21 nT at 2115 UT (Fig. 9). At the magnetic observatories in the auroral region, a burst of geomagnetic pulsations Psc 2–5 was recorded in the noon sector (Fig. 9). Such a burst is a conventional indicator for a sudden impulse or a storm sudden commencement.

An important feature of the variations in the SW density and in the IMF strength from observations by the Wind satellite far from the Earth and by the *Geotail* and *IMP-8* satellites near the magnetosphere is the

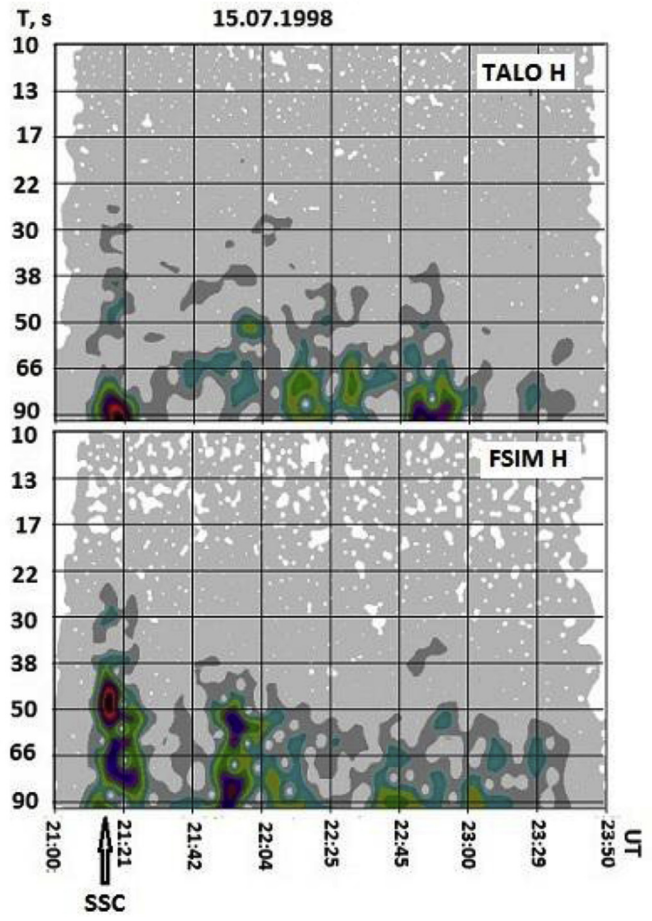

Fig. 9. Dynamic spectra of geomagnetic pulsations at the high-latitude observatories on dayside. The spectra show the Psc geomagnetic pulsations as an indicator of the sudden commencement at 21:15 UT. At the same time, a sharp jump of the H-component was recorded at the world network of magnetic observatories.

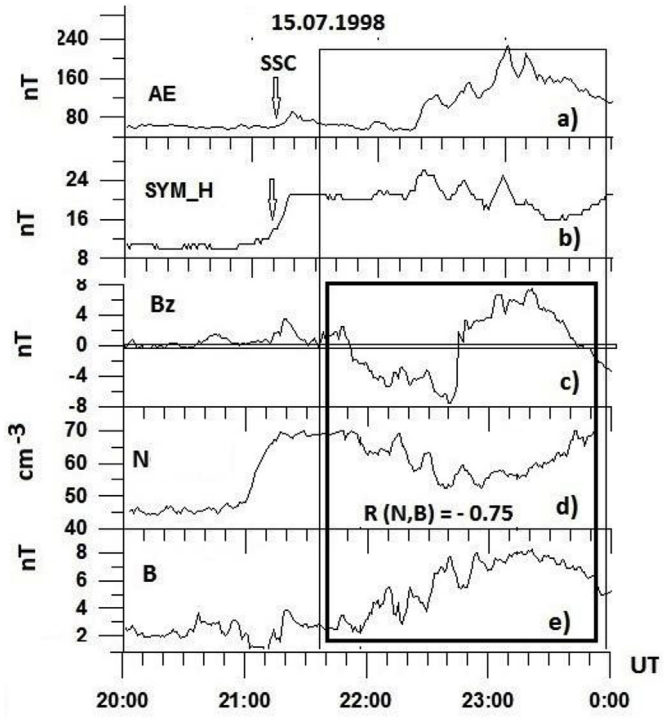

Fig. 10. Global response of the magnetosphere to the coupling with the diamagnetic structure inside HPS. a) variation in the AE index, b) variation in the SYM-H index, c) variation in the IMF Bz component, d) variation in the SW density, e) variation in the IMF modulus. The arrow marks the sudden commencement, the rectangle marks the time of the DS observation.

anti-correlation in their variations: the cross correlation coefficient of −0.75 is found within the interval from 2140 to 2359 UT on July 15, 1998. This enables to identify the variations in the SW parameters and in the IMF as a diamagnetic structure (the inner rectangle in Fig. 8 and the rectangle in Fig. 10).

Another feature of the 1900–2200 UT interval is a positive value of the IMF Bz component (0.60 ± 0.91 nT), Fig. 10c. This fact may be an argument in favor of the assumption that the source of the magnetospheric disturbances manifesting themselves in the AE index growth as many as 240 nT on July 15, 1998 and its modulation is an HPS diamagnetic structure.

Let us consider the features of the magnetospheric response at the noon meridian in the geosynchronous orbit and on the ground. As seen in Fig. 11b–d, a sharp increase in the SW density generates the storm sudden commencement recorded by the CANOPUS network of magnetometers located on the sunlit hemisphere. At the Fort Smith (FSMI) Observatory (Fig. 11b), located during the interaction near the noon meridian, as well as at other CANOPUS network observatories (Fig. 9), a train of geomagnetic pulsations Psc2-3 is recorded that is an indicator of a sudden commencement. After that, one observes the H-component growth with a superposition of long-period (10–15 min) oscillations. The *Geotail* detected similar periods in variations of the IMF strength and of the SW density.

GOES-9 was located near the noon meridian at this time and detected a sharp increase of geomagnetic field Bz component (Fig. 11c) and a sharp drop in the electron flux with E < 2 MeV (Fig. 11d). On both curves, one can see superimposed oscillations with a period, close to the oscillation period of the IMF modulus and of the SW density in the diamagnetic structure.

Let us consider the features of the magnetospheric disturbance evolution at the midnight meridian in the auroral oval (Fig. 12a). On the magnetogram from the Tromso Observatory (Φ = 69°.66, MLT = UT + 1.2) of the IMAGE meridional network, one can see the variations proper for an auroral substorm: there are three sequential sharp drops in the H-component. The sequence of bay-like recurrent disturbances 1–3 in Fig. 11a resembles saw teeth.

Troshichev and Janzhura (2012) studied such sequences of substorms and referred to the latter as sawtooth substorms. Based on analysis of the relation of recurrent bay-like magnetic disturbances in the auroral region to the dynamics of the auroras and fluxes of the particles in the geosynchronous orbit, the authors showed their difference from classical magnetospheric substorms: the absence of the auroral breakup. Another distinctive feature of such kind of substorms is the absence of the growth phase related to the energy accumulation at the magnetotail upon magnetic reconnection of the IMF and magnetospheric magnetic field lines. The latter is distinct characteristic of classical substorms, which is related to presence of a long-lasting southward IMF. We remind that, in the present case, magnetospheric disturbances were preceded by a long-lasting northward orientation of Bz.

We analyzed the causes of sawtooth substorms occurred in 62 cases cited in Tab. 7.10 from (Troshichev and Janzhura, 2012). All of these cases were shown to be a result of forcing on the magnetosphere from diamagnetic structures related either to the sporadic SW, or to the quasi-stationary slow SW. Thus, the results of data analysis presented for the July 15, 1998 event in Figs. 8, 10 and 11 are in good agreement with the conclusions by (Troshichev and Janzhura, 2012) about the existence of sawtooth substorms. Troshichev and Janzhura (2012) based their analysis on a great number of events. But, in addition to

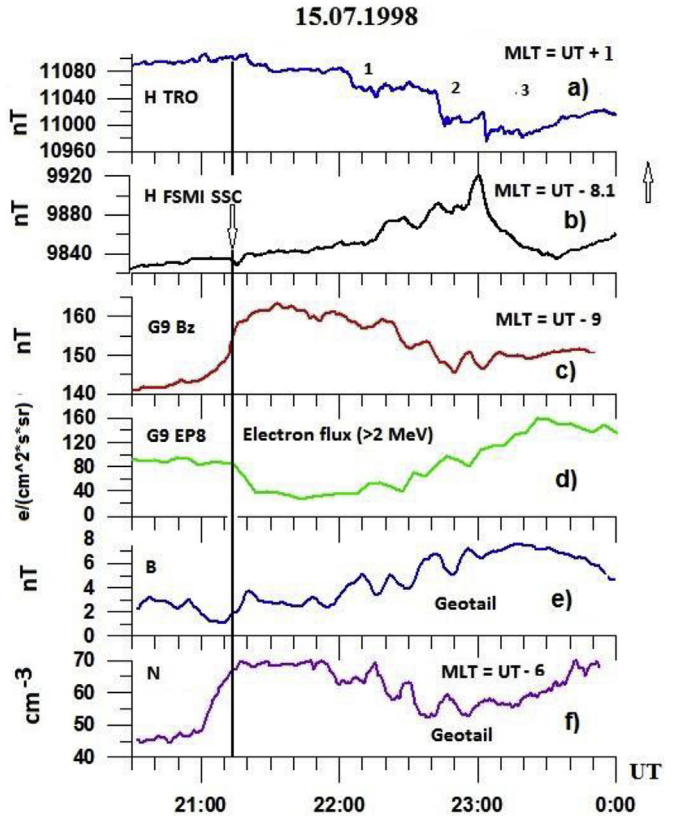

Fig. 11. Geomagnetic field modulation at nigh side (a) and day side (b) of the magnetosphere and in the geostationary orbit (c), modulation of the electron flux with > 2 MeV energies in the geostationary orbit by the IMF modulus variations (e) and by the SW density N (f).) a) a magnetogram fragment of the H-component from the Tromso Observatory at 66°. 64 in the premidnight sector, (b) a magnetogram fragment of the H-component from the FSMI Observatory at 67°.9 in the prenoon sector, (c) a magnetogram fragment of the Bz component in the geostationary orbit (GOES-8) in the noon sector, (d) electron flux variation in the geostationary orbit, e) IMF modulus variation at the Geotail, f) SW density measured by the Geotail satellite upstream of the magnetopause at ~20 Re at the ~15h meridian.

their conclusions, our analysis enables to determine the sources of sawtooth substorms. Those are the SW diamagnetic structures.

In addition to this conclusion, we note that the increase in the magnetospheric activity is also associated with a fast Bz turning southward against the increased SW pressure. I.e., probably, both these factors produce conditions for an abrupt enhancement of the energy transport into the magnetosphere. Thereby, the analysis of the observations on the Sun, in the solar wind, upstream of and inside the magnetosphere shows that an SW diamagnetic structure may be an energy source of a powerful magnetospheric disturbance: a magnetic storm and sawtooth substorms.

Another feature of the DS interaction with the magnetosphere is a global modulation of the geomagnetic field and particle fluxes in the geosynchronous orbit with a period close to the variation in the SW density and in the IMF strength in the diamagnetic structure. First of all, this modulation manifests itself in variations of the global geomagnetic activity planetary indices (AE, PC, and SYM-H) with the same period (Fig. 12a). The cross correlation coefficients between the index variations are equal to, respectively: R (AE, SYM-H) = 0.41, R (AE, PC) = 0.58, R (PC, SYM-H) = 0.43.

Another confirmation of the magnetosphere global modulation is yielded in Fig. 12b and c within the 2140–2305 UT interval. In this interval, one observes a train of long-period variations/oscillations of the equivalent ionospheric currents proportional to the mean inductive geomagnetic field over the observatories in all the latitude ranges from the northern polar cap to the southern one. The period of variations in the equivalent currents is close to the variations in the planetary indices of the geomagnetic activity and of the interplanetary electric field, and also correlates with the variation in the SW density (pressure) and in the IMF strength.

We provide another demonstration of generating a sawtooth substorm as a result of the DS interaction with the magnetosphere. Fig. 13 shows maps of vectors of the equivalent ionospheric currents for the moment of sudden commencement and for the moment of sawtooth substorm maximal evolution. The technique for calculation of the maps is described by (Parkhomov et al., 2015).

At the 2114 UT sudden commencement, the Sq current system is intensified on the sunlit hemisphere (Fig. 13a). At the midnight meridian (IMAGE network), at the auroral oval latitudes, there is an increase in the eastern current. This increase is determined by a growth in the vector length and by the prevailing eastern orientation of the vectors. At 2306 UT, one observes the maximal drop in the H-component at the Tromso Observatory (Fig. 11a). On the vector map, at auroral latitudes and near the midnight meridian, one can see (from the pattern of the vector distribution) an increase in the current and the prevailing western orientation of the vectors (Fig. 13b).

3.3. Inference to the DS related to the quasi-stationary slow SW

The diamagnetic structure related to the quasi-stationary slow SW generated a complex disturbance in the magnetosphere. The disturbance was modulated by the variations in the SW density and in the IMF strength with a ~10–15 min period, and includes:

1. A jump of and variations in the geomagnetic field and in the electron flux (E < 2 MeV) observed in the geostationary orbit in the noon sector.
2. A sudden commencement of the magnetic storm and synchronous oscillations of the magnetic field with a ~14-min period on the sunlit hemisphere.
3. A sawtooth substorm on the midnight side of the magnetosphere.
4. A global modulation of the magnetic activity and of the equivalent ionospheric currents.
5. The duration of the magnetospheric disturbance was determined by the time of structure interaction with the magnetosphere.

4. Conclusions

1. The interaction of the diamagnetic structures, having their sources on the Sun and transported to the Earth by the solar wind, with the magnetosphere generates substorm-like (sawtooth) magnetic disturbances in the nightside magnetosphere. The latter differ from classical substorms because of the absence of the growth phase and of the breakup.
2. The diamagnetic structures related to the quasi-stationary slow SW cause a global modulation of the magnetic activity and of the ionospheric currents with a period, close to the period of the variations in the SW plasma density and in the IMF strength inside the diamagnetic structure.

Acknowledgments

The authors are grateful to NASA CDAWEB for the possibility of using data on the parameters of the plasma and magnetic field measured aboard the Wind, Geotail, GOES_8, and Polar satellites. The authors thank Jan Mann and team members for data on geomagnetic field observations at the CARISMA and CANOPUS networks. The authors are also grateful to the proprietors of information for the possibility of using data of the Kyoto World Data Center for geomagnetism, the INTERMAGNET network, and the IMAGE and 210th Meridian

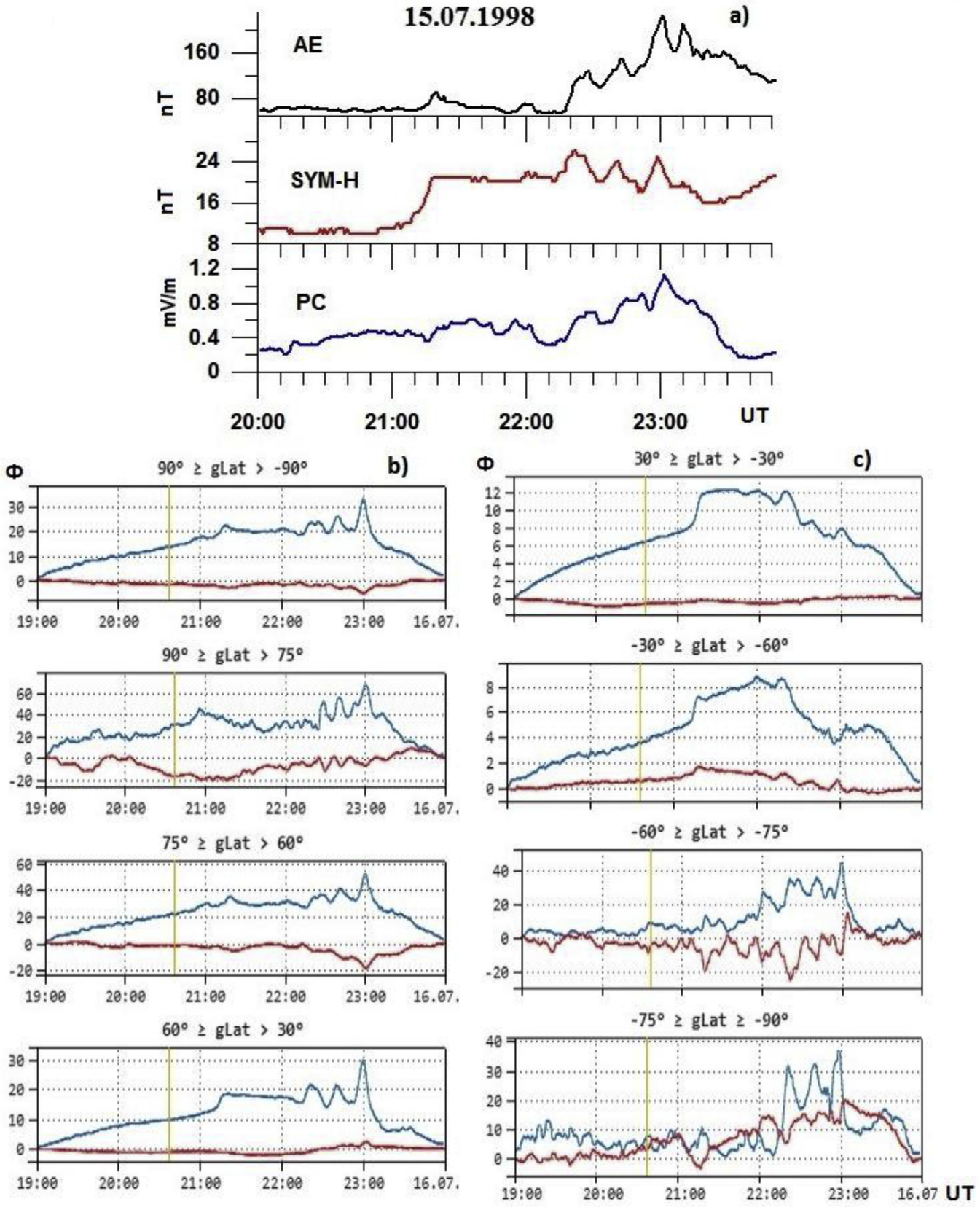

Fig. 12. An illustration of the global modulation of the ionosperic current systems. The modulation was caused by the July 15, 1998 DS coupling with the magnetosphere within 21:40–23:15 UT. a) Modulation of the magnetic activity planetary indices, b) variation in the mean strength induced by the equivalent ionospheric current at the observatories within the indicated range of geographic latitudes. The upper curve (dark blue line) is the Sm variation calculated by the strength values at the observatories within the indicated latitude ranges. The lower curve (red line) is the mean value for the variation in the vertical component at the observatories within the same latitude ranges.

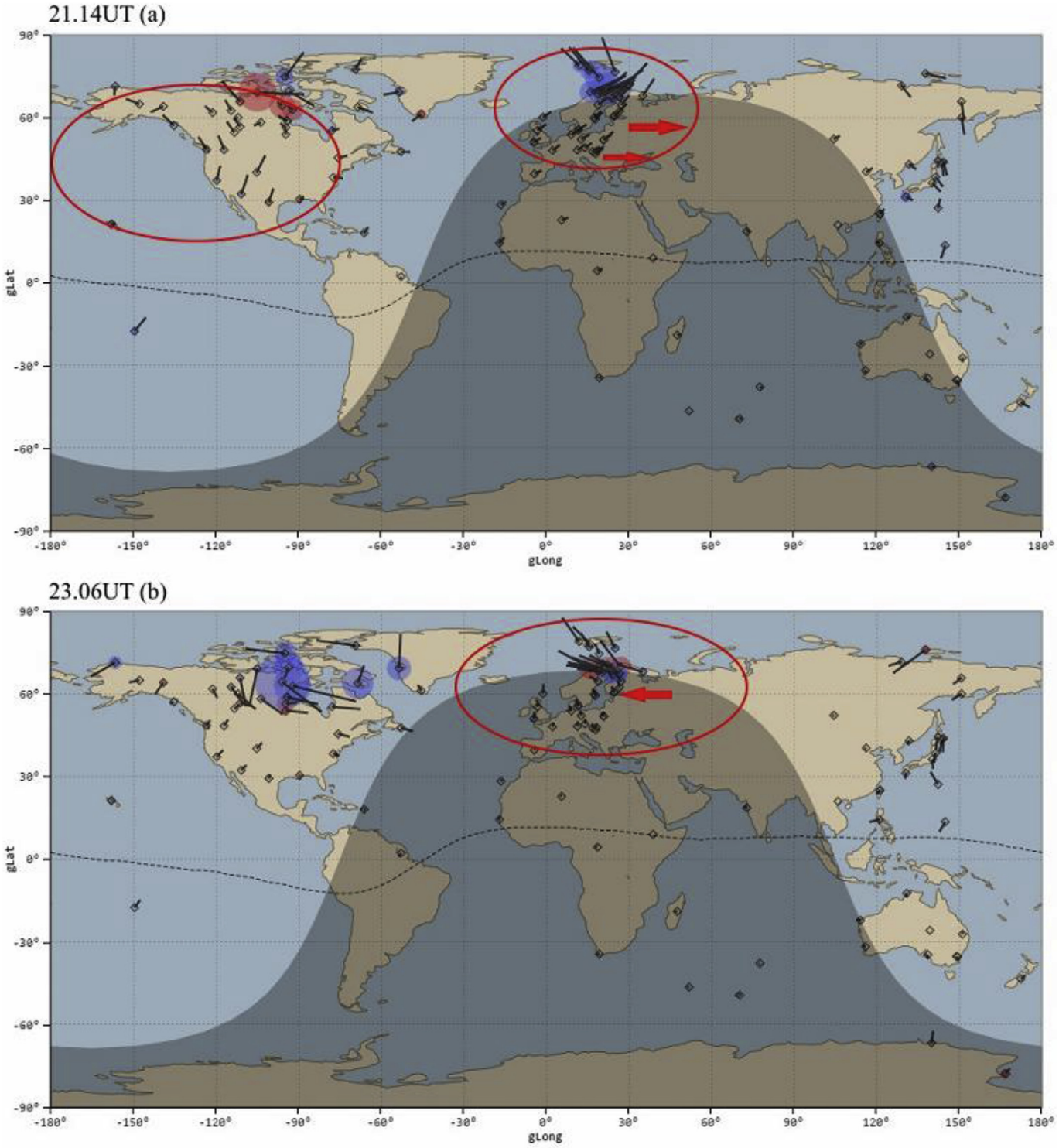

Fig. 13. Maps for vectors of the equivalent ionospheric currents from the Intermagnet network at the moment of the sudden commencement and at the moment of the substorm-like disturbance maximal evolution. On the map (a), the current at the midnight meridian is eastward; on the map (b), it is westward (substorm). The solid line is the magnetic equator. Symbol * is the subsolar point position.

meridional chains. The authors are grateful to Rudenko G.V. for calculating the position of the coronal holes and the neutral line of the global magnetic field of the Sun. We thank Yuri Kaplunenko for text translation in the English. The work of Borodkova N.L. was supported by project No. 16-12-10062 of Russian Science Foundation, Russia and the work of Dmitriev A.V. financially supported by the grant MOST-105-2111-M-008-018 of the Ministry of Science and Technology, Taiwan.

References

Akasofu, S.I., 1971. Polar and Magnetospheric Substorms. M. Mir., pp. 320.
Eselevich, M., Eselevich, V., Fujiki, K., 2007. Streamer belt and chains as the main sources of quasi-stationary slow solar wind. Sol. Phys. 240, 135–151. https://doi.org/10.1007/s11207-006-0197-z.
Eselevich, V.G., Fainshtein, V.G., 1991. The heliospheric current sheet (HCS) and high-speed solar wind: interaction effects. Planet. Space Si. 39 (N5), 737–744.
Eselevich, V.G., Fainshtein, V.G., Rudenko, G.V., 1999. Study of the structure of streamer

belts and chains in the solar corona. Solar Phys. 188 (2), 277.
Eselevich, M.V., Eselevich, V.G., 2005. Fractal structure of the heliospheric plasma sheetin the Earth's orbit. Geomagn. Aeron. 45 (3), 326–336.
Eselevich, M.V., Eselevich, V.G., 2006. Manifestations of the ray structure of the coronal streamer belt in the form of sharp peaks of the solar wind plasma density in the Earth orbit. Geomagn. Aeron. 46 (6), 770–782.
Henderson, M.G., Skoug, R., Donovan, E., Thomsen, M.F., Reeves, G.D., Denton, M.H., Singer, H.J., McPherron, R.L., Mende, S., Immel, T.J., Sigwarth, J.B., Frank, L.A., 2006. Substorms during the 10–11 August 2000 sawtooth event. J. Geophys. Res. 111, A06206. https://doi.org/10.1029/2005JA011366.
Ivanov, K., Bothmer, V., Cargill, P.J., Kharshiladze, A., Romashets, E.P., Veselovsky, I.S., 2002. Subsector structure of the interplanetary space. In: Proc. The Second Solar Cycle and Space whether Euroconference, pp. 317 Vicvo Equense (Italy).
Koskinen, H.E.J., Lopez, R.E., Pellinen, R., Pulkkinen, T.I., Baker, D.N., Bøsinger, T., 1993. Pseudobreakup and substorm growth phase in the ionosphere and magnetosphere. J. Geophys. Res. 98, 5801–5813. https://doi.org/10.1029/92JA02482.
Korzhov, N.P., 1977. Large-scale three-dimensional structure of the interplanetary magnetic field. Sol. Phys. 55, 505–517.
Lui, A.T.Y., 2001. Current controversies in magnetospheric physics. Rev. Geophys. 39 (4), 535–564. https://doi.org/10.1029/2000RG000090.
Parkhomov, V.A., Borodkova, N.L., Dmitriev, A.V., Klimov, P.M., Rakhmatulin, R.A., 2011. The role of solar wind pressure jumps in the initiation and control processes of magnetospheric substorms 2011. Geomagn. Aeron. 51 (7), 979–993.
Parkhomov, V.A., Borodkova, N.L., Eselevich, V.G., Eselevich, M.V., 2015. Abrupt changes of density in sporadic solar wind and their effect on Earth magnetosphere. Cosmic Res. 53 (6), 411–422.
Rouillard, A.P., Sheeley Jr., N.R., Cooper, T.J., et al., 2011. The solar original of small interplanetary tran-sients. Astrophys. J. https://doi.org/10.1088/0004-637X/734/1/7.
Sergeev, V., Nishimura, Y., Kubyshkina, M., Angelopoulos, V., Nakamura, R., Singer, H., 2012. Magnetospheric location of the equatorward prebreakup arc. J. Geophys. Res. 117, A01212. https://doi.org/10.1029/2011JA017154.
Schwenn, R., Dal Lago, A., Huttunen, E., et al., 2005. The association of coronal mass ejections with their effects near the Earth. Ann. Geophys. V. 23, 1033.
Svalgaard, L.J., Wilcox, W., Duvall, T.L., 1974. A model combining the solar magnetic field. Sol. Phys. 37, 157–172.
Troshichev, O.A., Peter, Stauning, Kan, Liou, Reeves, Geoff, 2010. Saw-tooth substorms: inconsistency of repetitive bay-like magnetic disturbances with behavior of aurora. In: EGU General Assembly 2010. Geophysical Research Abstracts, vol 12 EGU2010-3602.
Troshichev, O.A., Janzhura, A., 2012. Space Weather Monitoring by Ground-based Means: PC Index. Springer Verlaghttps://doi.org/10.1007/978-3-642-16803-1.
Tsegmed, B., 2002. Generation of a burst of geomagnetic pulsations in the 1–3 Hz frequency range in the daytime sector as a result of dramatic increases in the solar wind dynamic pressure. Geomagn. Aeron. 51 (8), 1138–1145.
Wang, Y.M., Sheeley, N.R., Rich, N.B., 2007. Coronal pseudostreamers. Astrophys. J. 685, 1340–1348.
Zhou, X., Tsurutani, B.T., 1999. Rapid intensification and propagation of the dayside aurora: large scale interplanetary pressure pulses (fast shocks). Geophys. Res. Lett. 26 (8), 1097–1100.
Zhou, X., Tsurutani, B.T., 2001. Interplanetary shock triggering of nightside geomagnetic activity: sub-storms, pseudobreakups and quisescent events. J. Geophys. Res. 106 (A9), 18957–18967.
Zhou, X., Xu-Zxi, Zhou, Angelopolus, V., et al., 2013. Interplanetary shock-induced current sheet dis-turbances leading to auroral activations: THEMIS observations. J. Geophys. Res. V. 118, 3173. https://doi.org/10.1002/igra.50175.